Microwave Zeeman Spectrum of Atomic Chlorine*†

V. BELTRAN-LOPEZ‡ AND H. G. ROBINSON
Gibbs Physics Laboratory, Yale University, New Haven, Connecticut
(Received February 17, 1961)

The microwave spectrum of atomic chlorine has been observed at 9190 Mc/sec in the products of an rf electrodeless discharge. Of the twelve allowed transitions per isotope, $\Delta M_I=0$, $\Delta M=\pm 1$, five arising from Cl^{35} and two from Cl^{37} have been measured. Using a nonrelativistic Hamiltonian, analysis of the data yields $-g_J(\mathrm{Cl};{}^2P_{\frac{3}{2}})/g_p=438.50415\pm 0.00063$, where g_p is the proton gyromagnetic ratio in a cylindrical sample of mineral oil. This result can be transformed to $g_J(\mathrm{Cl};{}^2P_{\frac{3}{2}})/g_J(\mathrm{D})=0.666201\pm 0.000002$. A calculation of the g_J(Cl)-isotope effect shows that it should not be observable in the present experiment. Estimates of the atom-atom and atom-molecule hard-sphere collision cross sections are made from measurements of linewidth and line intensity.

1. INTRODUCTION

THE excellent agreement between the theoretically computed and experimentally determined electronic g factors for fluorine[1] produced incentive for conducting a similar experiment for the heavier halogen, chlorine. This paper describes the experimental and analytical techniques used in the determination of $g_J(\mathrm{Cl};{}^2P_{\frac{3}{2}})$. It is hoped that when suitably accurate wave functions are available, the results presented here will be of value in further testing the theory of atomic magnetism.

2. APPARATUS

The microwave paramagnetic resonance spectrometer used in this experiment was originally developed by Beringer and Heald[2] and later modified for experiments on oxygen[3] and fluorine.[1] A description of the apparatus is given in references 1–3. The scheme for producing the atomic vapor to be studied is similar to that employed for fluorine. Chlorine gas bled into the pumping line passing through the microwave cavity was dissociated directly above the cavity by means of a 50-w electrodeless rf discharge. A 1-mm i.d. constriction in the tubing just below the discharge allowed the attainment of a lower pressure (80μ Hg) in the cavity region, thus reducing pressure broadening of the observed absorption line while permitting a higher pressure in the discharge region for optimum atom production. No wall coating was applied to the tube. A 2-liter liquid air trap on the downstream side of the cavity was used to remove the pumped chlorine gas. The Pound-stabilized klystron providing the microwave transition energy was continuously monitored against a harmonic of the laboratory cesium beam frequency standard.[4] In this way the transition frequency was measured to 0.1 ppm. The applied magnetic field was regulated by a proton resonance probe. The proton resonance oscillator was locked to the desired frequency synthesized from the laboratory frequency standard and a BC-221 frequency meter. A field stability of 0.1 ppm was achieved at the position of the regulating probe.

3. EXPERIMENTAL PROCEDURE

Before taking any measurements on a given transition, the microwave cavity was removed and the magnetic field in the 2-cm^3 sample region was shimmed to a homogeneity of at least 3 ppm. The field was plotted by a second proton probe of 30-mm^3 volume. A final check on the field homogeneity with the cavity in place was made preceding each run by recording the proton resonance, using a larger field-calibrating probe, probe I, positioned to occupy the volume in the cavity seen by the absorbing atom vapor. Since the microwave magnetic field and proton-resonance probe rf magnetic field will not have the same spatial distributions over the sample volume, the apparent center of one resonance may not correspond with that of the other resonance. To estimate the size of such an effect, another calibrating probe, probe II, of smaller diameter was used. The field as measured by probe I was now plotted against the field-regulating probe. After exchanging probe I for probe II, the plot was repeated. It was found that when the proton resonance was symmetrical and the field gradient less than 3 ppm, the two plots coincided to within 1 ppm. Thus, any error arising from differences in $\int H_{\mathrm{rf}}{}^2 dV_{\mathrm{sample}}$ for chlorine atoms and nuclear magnetic resonance protons lies within the field inhomogeneity. Figure 1 shows the dimensions of the calibrating probes.

The process of taking data consisted essentially of plotting in a point-by-point fashion the quasi-derivative absorption line as a function of the field-regulating probe frequency while keeping the klystron frequency fixed. Thus a knowledge of the field differential between the regulating probe and the sample was necessary. This was measured by means of calibrating probe I both before and after a microwave run. Data were accepted only when two such field-calibrating runs

* This work supported in part by the Office of Naval Research.
† Submitted by V. Beltran-Lopez in partial fulfillment of the Ph.D. thesis requirement at Yale University, New Haven, Connecticut.
‡ General Electric Fellow 1960–61.
[1] H. E. Radford, V. W. Hughes, and V. Beltran-Lopez, Phys. Rev. **122**, 153 (1961).
[2] R. Beringer and M. A. Heald, Phys. Rev. **95**, 1474 (1954).
[3] H. E. Radford and V. W. Hughes, Phys. Rev. **114**, 1274 (1959).
[4] National Company Atomichron.

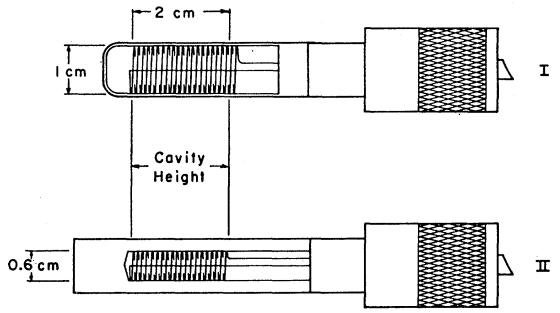

FIG. 1. Field-calibrating proton probes referred to as I, II in text.

agreed to within the measured field inhomogeneity. The cavity resonance frequency was measured before and after each run since, if the klystron and cavity are not tuned to the same frequency, the apparent center of the observed resonance will shift an amount proportional to $d\nu=(\nu_{\text{cavity}}-\nu_{\text{klystron}})$. For conditions encountered in this experiment, this effect amounted to an apparent shift of $d\nu/5$. In typical runs, this shift was $\leqslant 10^{-2}$ ppm. The points obtained by the method described above for a given run were plotted as shown in Fig. 2. The line center, chosen as the crossover point for a symmetric line, could then be assigned a value of magnetic field in terms of the corresponding proton resonance frequency.

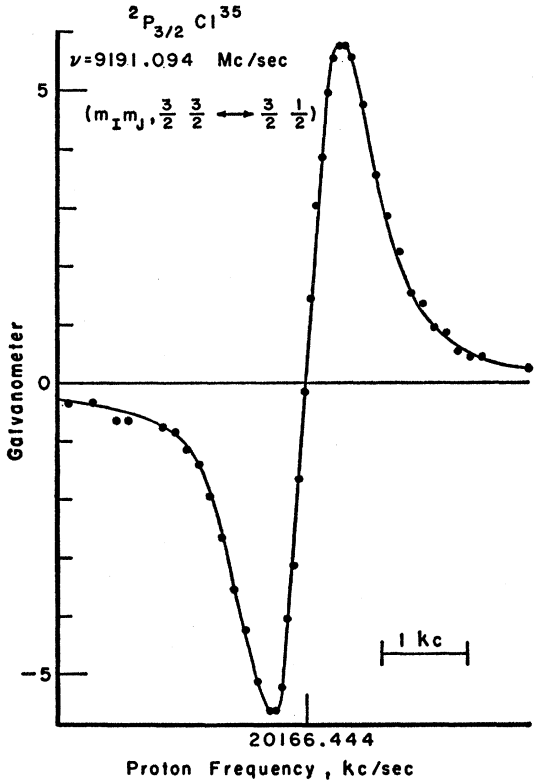

FIG. 2. Typical absorption line in chlorine atomic vapor.

4. THEORY

The ground term of atomic chlorine is an inverted ^2P, the $^2P_{\frac{1}{2}}$ level lying 2641×10^4 Mc/sec above the $^2P_{\frac{3}{2}}$ level.[5] Both isotopes Cl^{35}, Cl^{37} have a nuclear spin of $\frac{3}{2}$, and hence magnetic and electric hyperfine interactions are present. As a result, the magnetic dipole selection rules $\Delta M_I=0$, $\Delta M_J=\pm1$ allow a total of 12 resolved transitions at a nominal frequency of 9190 Mc/sec among the 16 nondegenerate ground-state energy levels.

Since the chlorine atom has a p^5 electron configuration, if LS coupling holds it can be treated as a closed shell plus one "positive p electron." The use of a nonrelativistic, single-electron Hamiltonian may then be possible. A relativistic treatment for the single electron has been considered by several authors.[6–9] For the energy levels of chlorine with LS coupling, relativistic corrections not absorbed by g_J and the hyperfine coupling constants a, b amount to $\leqslant 0.1$ ppm. Since a precision on the order of 1 ppm was expected in this experiment, the choice of the nonrelativistic treatment appeared reasonable. The internal consistency of the results can be used in judging the validity of this approach.

The experimental data were analyzed using the following Hamiltonian:

$$\mathcal{H}=\mathcal{H}_0+\mu_0(g_L\mathbf{L}+g_s\mathbf{S})\cdot\mathbf{H}_0+\mu_0 g_I\mathbf{I}\cdot(\mathbf{H}_0+\mathbf{H}_e)+\mathcal{H}_{\text{el}}, \quad (1)$$

where $\mathcal{H}_0$ is that part which has no orientational dependence; $\mathbf{H}_0$ is the applied magnetic field; $\mathbf{H}_e$ is the magnetic field at the nucleus caused by the electrons; and $\mathcal{H}_{\text{el}}$ is the difference between the true electrostatic interaction and the interaction between the electrons

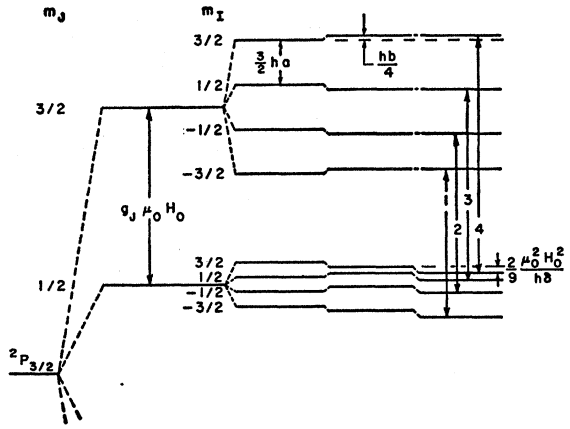

FIG. 3. Schematic representation of the energy levels of a ground-state chlorine atom in an external magnetic field. Energy levels associated with $M_J=-\frac{1}{2}$, $-\frac{3}{2}$ are not shown.

[5] L. Davis, Jr., B. T. Feld, C. W. Zabel, and J. R. Zacharias, Phys. Rev. **76**, 1076 (1949).
[6] G. Breit and Lawrence A. Wills, Phys. Rev. **44**, 470 (1933).
[7] W. W. Clendenin, Phys. Rev. **94**, 1590 (1954).
[8] Charles Schwartz, Phys. Rev. **97**, 380 (1955).
[9] H. B. G. Casimir, *On the Interactions Between Atomic Nuclei and Electrons* (Teyler's Tweede Genootschap, Haarlem, 1936).

and a nuclear point charge. This scheme of writing the Hamiltonian preserves any possible contributions off-diagonal in J. The desired energy levels can be obtained by treating off-diagonal hfs contributions separately and working at first with the Hamiltonian

$$\mathcal{H}=\mathcal{H}_0+\mu_0(g_L\mathbf{L}+g_s\mathbf{S})\cdot\mathbf{H}_0 +\mu_0 g_I\mathbf{I}\cdot\mathbf{H}_0+ha\mathbf{I}\cdot\mathbf{J}+hbQ_{\rm op}. \quad (2)$$

The values used for the hfs coupling constants a, b were those of Holloway, Aubrey, and King.[10] Figure 3 shows schematically the energy levels of chlorine in a high magnetic field. The shift of the $M_J=\pm\frac{1}{2}$ levels, $(2\mu_0^2H_0^2/9h\delta)\approx 40$ ppm, results from the mixing of the $^2P_{\frac{1}{2}}$ and $^2P_{\frac{3}{2}}$ states by the applied magnetic field. The spectrum of the allowed transitions for each isotope is shown in Fig. 4.

At a resonance frequency of 9190 Mc/sec the applied magnetic field essentially decouples $\mathbf{J}$ and $\mathbf{I}$ ($a\simeq 200$ Mc/sec). Thus an appropriate representation is (JIM_JM_I). Labeling with M_FM_J, where $M_F=M_J+M_I$, the secular determinant breaks up into subdeterminants along the diagonal. The determinant for the P-doublet level complex consisting of 24 rows and 24 columns can be reduced to 16×16 by eliminating elements off-diagonal in J. This was done by adding appropriate multiples of rows and columns. All $^2P_{\frac{1}{2}}$ levels were assumed to lie an amount $h\delta$ above the $^2P_{\frac{3}{2}}$ levels. The error resulting from this approximation

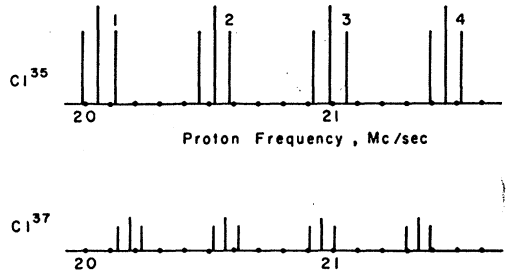

FIG. 4. High-field microwave Zeeman spectrum of chlorine at 9100 Mc/sec. The four labeled resonances correspond to the numbered transitions shown in Fig. 3.

arises from omission of terms in $1/\delta^2$, where δ is the doublet separation. Figure 5 shows the secular determinant $(1/ha)|\mathcal{H}_{M_FM_J}|$ of Eq. (2) correct to terms through order $1/\delta$ after reduction of the $^2P_{\frac{1}{2}}$ elements. An exact solution (through order $1/\delta$) was feasible for the energy levels $(M_I,M_J)=\pm(\frac{3}{2},\frac{3}{2})$, $\pm(\frac{3}{2},\frac{1}{2})$, and $\pm(\frac{1}{2},\frac{3}{2})$. For the observed transition $(M_I;M_J\leftrightarrow M_{J'})=(\frac{3}{2};\frac{3}{2}\leftrightarrow\frac{1}{2})$ it was then possible to obtain a polynomial in the dimensionless parameter $x=\mu_0g_JH_0/ha$ without introducing any significant additional approximations. In the case of the more unwieldy transitions, pertinent energies were expressed as series in powers of x. These expansions were carried out through terms equivalent to those obtained by a fourth-order perturbation treatment. Neglected terms are expected to contribute

The Secular Determinant of $\frac{\mathcal{H}}{ha}$

$$X=\frac{\mu_0 g_J H_0}{ha}\left\{m_J+\frac{g_I}{g_J}m_I\right\}$$

$$\alpha=\frac{b}{a}\ ;\quad \gamma=\frac{a}{8\delta}\left(\frac{\mu_0 g_J H_0}{ha}\right)^2$$

m_F	m_J																
-3	-3/2	$X+\frac{9+\alpha}{4}-E$	•	•	•	•	•	•	•	•	•	•	•	•	•	•	•
-2	-3/2	•	$X+\frac{3-\alpha}{4}-E$	$\frac{3+\alpha}{2}$	•	•	•	•	•	•	•	•	•	•	•	•	•
	-1/2	•	$\frac{3+\alpha}{2}$	$X+\frac{3-\alpha}{4}-\gamma-E$	•	•	•	•	•	•	•	•	•	•	•	•	•
-1	-3/2	•	•	•	$X-\frac{3+\alpha}{4}-E$	$\sqrt{3}$	$\frac{\alpha}{2}$	•	•	•	•	•	•	•	•	•	•
	-1/2	•	•	•	$\sqrt{3}$	$X+\frac{1+\alpha}{4}-\gamma-E$	$\sqrt{3}$	•	•	•	•	•	•	•	•	•	•
	1/2	•	•	•	$\frac{\alpha}{2}$	$\sqrt{3}$	$X-\frac{3+\alpha}{4}-\gamma-E$	•	•	•	•	•	•	•	•	•	•
0	-3/2	•	•	•	•	•	•	$X-\frac{9-\alpha}{4}-E$	$\frac{3-\alpha}{2}$	$\frac{\alpha}{2}$	•	•	•	•	•	•	•
	-1/2	•	•	•	•	•	•	$\frac{3-\alpha}{2}$	$X-\frac{1-\alpha}{4}-\gamma-E$	2	$\frac{\alpha}{2}$	•	•	•	•	•	•
	1/2	•	•	•	•	•	•	$\frac{\alpha}{2}$	2	$X-\frac{1-\alpha}{4}-\gamma-E$	$\frac{3-\alpha}{2}$	•	•	•	•	•	•
	3/2	•	•	•	•	•	•	•	$\frac{\alpha}{2}$	$\frac{3-\alpha}{2}$	$X-\frac{9-\alpha}{4}-E$	•	•	•	•	•	•
1	-1/2	•	•	•	•	•	•	•	•	•	•	$X-\frac{3+\alpha}{4}-\gamma-E$	$\sqrt{3}$	$\frac{\alpha}{2}$	•	•	•
	1/2	•	•	•	•	•	•	•	•	•	•	$\sqrt{3}$	$X+\frac{1+\alpha}{4}-\gamma-E$	$\sqrt{3}$	•	•	•
	3/2	•	•	•	•	•	•	•	•	•	•	$\frac{\alpha}{2}$	$\sqrt{3}$	$X-\frac{3+\alpha}{4}-E$	•	•	•
2	3/2	•	•	•	•	•	•	•	•	•	•	•	•	•	$X+\frac{3-\alpha}{4}-E$	$\frac{3+\alpha}{2}$	•
	1/2	•	•	•	•	•	•	•	•	•	•	•	•	•	$\frac{3+\alpha}{2}$	$X+\frac{3-\alpha}{4}-\gamma-E$	•
3	3/2	•	•	•	•	•	•	•	•	•	•	•	•	•	•	•	$X+\frac{9+\alpha}{4}-E$

FIG. 5. The secular determinant of $\mathcal{H}/ha$ of Eq. (2) correct to terms through order $1/\delta$ after reduction of the $^2P_{\frac{1}{2}}$ elements.

[10] J. H. Holloway, B. B. Aubrey, and J. G. King, Massachusetts Institute of Technology Quarterly Progress Report, Research Laboratory for Electronics, April 15, 1956 (unpublished).

TABLE I. Solutions of Eq. (2) for selected transitions as polynomials in x; $x=\mu_0 g_J H_0/ha$. Use upper sign for $M_I=\frac{1}{2}$ and lower sign for $M_I=-\frac{1}{2}$.

M_I;	$M_J \leftrightarrow M_{J'}$	Polynomial
$\frac{3}{2}$;	$\frac{3}{2}\leftrightarrow\frac{1}{2}$	$\left(\frac{g_I}{g_J}\right)\left(\frac{a}{8\delta}\right)x^3+\left[\frac{g_I}{g_J}\frac{a}{8\delta}\left(\frac{\nu}{a}-\frac{3+\alpha}{2}\right)\right]x^2-\left(1+\frac{g_I}{g_J}\right)\left(\frac{\nu}{a}-\frac{3+\alpha}{2}\right)x+\left[\frac{\nu}{a}-(3+\alpha)\right]\frac{\nu}{a}=0$
$\frac{1}{2}$;	$\frac{3}{2}\leftrightarrow\frac{1}{2}$	$\pm\frac{ax^2}{8\delta}+x-\left(\frac{\nu}{a}\mp\frac{1-\alpha}{2}\right)+\frac{(3+\alpha)^2}{(1-g_I/g_J)}\left(\frac{1}{x}\right)\pm\frac{6(1+\alpha)}{(1-g_I/g_J)^2}\left(\frac{1}{x^2}\right)-\frac{(3+\alpha)^4}{16(1-g_I/g_J)^3}\left(\frac{1}{x^3}\right)=0$
$-\frac{1}{2}$;	$-\frac{1}{2}\leftrightarrow-\frac{3}{2}$	
$\pm\frac{1}{2}$;	$\frac{1}{2}\leftrightarrow-\frac{1}{2}$	$x-\left(\frac{\nu}{a}\mp\frac{1}{2}\right)+\frac{7/4+3\alpha/2-\alpha^2/8}{(1-g_I/g_J)}\left(\frac{1}{x}\right)\mp\frac{6(1+\alpha)-(6-\alpha)^2/8}{(1-g_I/g_J)^2}\left(\frac{1}{x^2}\right)-\frac{319+252\alpha}{32}\left(\frac{1}{x^3}\right)=0$

corrections on the order of 0.1 ppm. For the 5 transitions measured, the formulas derived as discussed above are given in Table I.

For a selected transition, an iterative method can be used to solve the corresponding equation given in Table I for the value of x. In the case of the $(\frac{3}{2};\frac{3}{2}\leftrightarrow\frac{1}{2})$ transition, it was possible to derive an approximate solution accurate to 0.2 ppm:

$$x=k\left[1-\frac{g_I}{g_J}\left(1-\frac{2ak}{2\nu-(3+\alpha)a}\right)\right]\left[1-\frac{ak}{8\delta}\right], \qquad (3)$$

where

$$k=\frac{\nu-(3+\alpha)a}{2\nu-(3+\alpha)a}\left(\frac{2\nu}{a}\right); \quad \alpha=b/a.$$

The treatment of remaining hfs contributions was as follows: After including matrix elements of $\mu_0 g_I(\mathbf{I}\cdot\mathbf{H}_e)$ and $\mathcal{H}_{el}$ off-diagonal[11] in J in the 24×24 secular determinant, a subsequent reduction to a 16×16 determinant showed that only hfs elements diagonal in M_J, M_I contribute significant corrections to the energy of the levels. These corrections, to be added to the values of x obtained from the solutions of the equations in Table I, are given in Table II. Here b is the usual quadrupole coupling constant and a''' is the off-diagonal magnetic hfs coupling constant defined by

$$a'''=-\frac{\mu_I}{I}\frac{(JM_J|(\mathbf{H}_e)_z|J-1\,M_J)}{(2J-1)^{\frac{1}{2}}}; \quad M_J=J-1. \qquad (4)$$

The ratio a'''/a can be computed using single p-electron wave functions. This result,[12] $a'''/a=-5/16$, together with the known value of a permits the choice of a reasonable trial value for a'''. No readjustment was found necessary for fitting theory and experiment within the experimental error.

[11] Matrix elements of $\mathcal{H}_{el}$ given by Schwartz[8] in the (FM_F) representation were transformed to the $(M_J M_I)$ representation. In the formalism of Schwartz, no explicit identification of the off-diagonal electric hfs coupling constant b''' is made. The matrix elements are displayed in terms of the quadrupole coupling constant b. Hence b''' does not appear in Table II.

[12] The sign of a''', here taken to be consistent with that of Casimir,[9] is determined by the choice of the phase of the wave functions. This choice is such that the sign of the matrix element $(LSJM_J|L_z|LS\,J-1\,M_J)$ is negative for $M_J=J-1$.

5. RESULTS

Having determined a value of x for a given microwave transition frequency and applied magnetic field, the ratio $g_J(\mathrm{Cl})/g_p$ follows as the primary experimental result. Here g_p refers to protons in the mineral oil of probe I, Fig. 1. For Cl^{35}, 28 measurements were made on the 5 transitions indicated in Table I. A histogram of $g_J(Cl^{35})/g_p$ determinations reduced from these data is shown in Fig. 6. The transitions $(M_I, M_J\leftrightarrow M_{J'})=(\frac{3}{2},\frac{3}{2}\leftrightarrow\frac{1}{2})$ and $(\frac{1}{2},\frac{1}{2}\leftrightarrow-\frac{1}{2})$ were also measured for Cl^{37}. The following values were found:

$$-g_J(Cl^{35};{}^2P_{\frac{3}{2}})/g_p=438.5042\pm0.0006,$$
$$-g_J(Cl^{37};{}^2P_{\frac{3}{2}})/g_p=438.5038\pm0.0008.$$

The errors quoted were taken as $\pm$ the half-widths at half heights of the respective histograms. A weighted average of the $g_J(\mathrm{Cl})/g_p$ ratios for the chlorine isotopes gives

$$-g_J(\mathrm{Cl};{}^2P_{\frac{3}{2}})g_p=438.50415\pm0.00063.$$

This ratio can be transformed to $g_J(\mathrm{Cl})/g_J(\mathrm{D})$ by using the Geiger, Hughes, and Radford[13] measurement of $g_J(\mathrm{D})/g_p$. Thus,

$$g_J(\mathrm{Cl};{}^2P_{\frac{3}{2}})/g_J(\mathrm{D})=0.666201\pm0.000002.$$

Since the scatter of the g_J values for different transitions reflects the uncertainty in the theory, and since the width of the histogram for all measured Cl^{35} transitions (Fig. 6) is comparable to the width of that for a single transition, the Hamiltonian given in Eq. (1) is apparently adequate for the precision attained in this experiment.

The question of observability of a $g_J(\mathrm{Cl})$-isotope effect arises. A nuclear mass dependence is expected, since the orbital g factor, g_L, is affected by the motion of the nucleus. The general theory of this effect has been given by Phillips.[14] Where M_i is the nuclear mass and m is the electron mass, the order of magnitude of such an effect for ${}^2P_{\frac{3}{2}}$ state is given by

$$|g_J(M_1)/g_J(M_2)|\approx\tfrac{1}{2}(m\Delta M/M_1M_2). \qquad (5)$$

[13] J. S. Geiger, V. W. Hughes, and H. E. Radford, Phys. Rev. **105**, 183 (1957).

[14] M. Phillips, Phys. Rev. **76**, 1803 (1949).

TABLE II. hfs corrections to x off-diagonal in J.

M_I;	$M_J \leftrightarrow M_{J'}$	Δx
$\frac{3}{2}$;	$\frac{3}{2} \leftrightarrow \frac{1}{2}$	$-3a'''x/2\delta+bx/4\delta$
$\frac{1}{2}$;	$\frac{3}{2} \leftrightarrow \frac{1}{2}$	$-a'''x/2\delta-bx/4\delta$
$-\frac{1}{2}$;	$-\frac{1}{2} \leftrightarrow -\frac{3}{2}$	
$\pm\frac{1}{2}$;	$\frac{1}{2} \leftrightarrow -\frac{1}{2}$	$+bx/2\delta$

Following the treatment by Abragam and VanVleck,[15] a calculation using Slater wave functions[16] gives $g_J(\mathrm{Cl}^{35})/g_J(\mathrm{Cl}^{37}) \approx -0.1$ ppm. Apparently then, no g_J-isotope effect should be observable in the present experiment.

The chlorine g factor itself can be written

$$g_J(\mathrm{Cl}) = \frac{g_J(\mathrm{Cl})}{g_p} \cdot \frac{1}{g_s/g_p} \cdot g_s. \tag{6}$$

The experimental value[13] $g_J(\mathrm{D})/g_p$ was transformed to g_s/g_p. This ratio, $g_s/g_p = -658.2279 \pm 0.0008$, and the g factor of the free electron,[17] $g_s = 2.0023192$, give

$$g_J(\mathrm{Cl}; {}^2P_{\frac{3}{2}}) = 1.333923 \pm 0.000003.$$

The error quoted includes the uncertainty in the ratio g_s/g_p.

6. COMPARISON WITH OTHER MEASUREMENTS

The change in the above value of $g_J(\mathrm{Cl})$ from that reported earlier[18] resulted wholly from refinement in the theory. Independent determinations have been reported by Wolga and Strandberg,[19] $[g_J(\mathrm{Cl})]_{\mathrm{WS}} = 1.33376 \pm 0.00007$; and by Harvey, Kamper, and Lea,[20] $[g_J(\mathrm{Cl})]_{\mathrm{HKL}} = 1.3339275 \pm 0.0000030$, with $g_J(\mathrm{Cl})/g_p = 438.5048 \pm 0.0007$. In view of the apparent difference in the g factor as determined by independent work, a brief discussion of possible causes follows[21]. The proton environment in the HKL experiment was a 0.163-molar solution of nickel sulfate. In deriving $g_J(\mathrm{Cl})$, HKL used the Koenig, Prodell, Kusch[22] value for $g_J(\mathrm{H})/g_p$ (spherical mineral oil sample). They then transformed this ratio to that for an H_2O sample by a correction of 3.4 ppm.[23] No further correction was applied, since the bulk diamagnetism of H_2O was cancelled by the paramagnetism of the nickel sulfate. For comparison

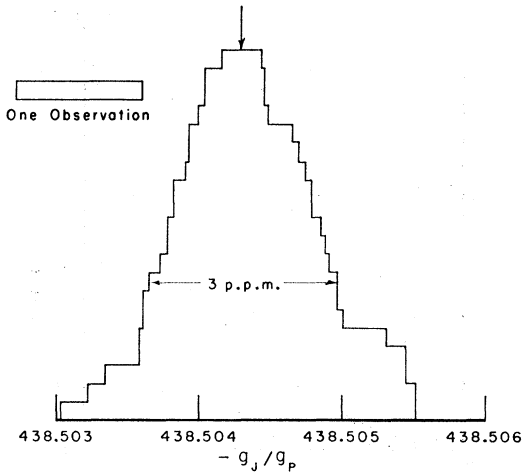

FIG. 6. Histogram of 28 determinations of $g_J(\mathrm{Cl}^{35})/g_p$ from five transitions in Cl^{35}.

with the result obtained in this paper, $[g_J(\mathrm{Cl})]_{\mathrm{BR}} = 1.333923 \pm 0.000003$, $g_J(\mathrm{Cl})$ was calculated [Eq. (6)] using the HKL value of $g_J(\mathrm{Cl})/g_p$ and $g_J(\mathrm{D})/g_p$ instead of $g_J(\mathrm{H})/g_p$,[22] both referred to the same proton geometry. Thus, $[g_J(\mathrm{Cl})]_{\mathrm{HKL}}' = 1.3339294 \pm 0.0000030$. Thomas,[23] using Petrolatum USP-light, and Gutowsky and McClure,[24] using Nujol, have reported g_p values for these two mineral oils which differ by 2.1 ppm referred to H_2 gas. This difference is of proper size to cause agreement between the HKL and BR results. However, application of such a correction cannot here be justified. In order to avoid complication in transforming $g_J(\mathrm{Cl})/g_p$ to $g_J(\mathrm{Cl})$, BR used the same mineral oil and sample geometry as was used in measuring $g_J(\mathrm{D})/g_p$. Thus, shape factor or sample difference corrections should not enter. As a check, a redetermination of $g_J(\mathrm{O})/g_p$ was made; the result agreed with that obtained previously[3] to within 1 ppm.

Although a detailed comparison of the theories used by HKL and BR was not made, the basic assumptions are evidently the same. A mutual exchange of data and subsequent calculation showed a difference of 1 ppm in the values of $g_J(\mathrm{Cl})$. This was true even for one of the theoretically simplest transitions, $(\frac{3}{2}; \frac{3}{2} \leftrightarrow \frac{1}{2})$. The cause of the discrepancy is not known at present.

Theoretical calculations of g_J values for the halogens have been presented by HKL. For chlorine, using presently available wave functions, satisfactory agreement with experiment was found to within the limits of accuracy of theory, ≈ 10 ppm.

7. COLLISION CROSS SECTIONS

By observing under constant pressure the absorption linewidth while varying the number of absorbing atoms, one obtains information leading to a value for atom-

[15] A. Abragam and J. H. VanVleck, Phys. Rev. **92**, 1448 (1953).
[16] J. C. Slater, Phys. Rev. **36**, 57 (1930).
[17] C. M. Sommerfield, Phys. Rev. **107**, 328 (1957).
[18] V. Beltran-Lopez and H. G. Robinson, Bull. Am. Phys. Soc. **5**, 273 (1960).
[19] G. Wolga and M. W. P. Strandberg, Bull. Am. Phys. Soc. **4**, 153 (1959); referred to as WS.
[20] J. S. M. Harvey, R. A. Kamper, and K. R. Lea, Proc. Phys. Soc. (London) **76**, 979 (1960); referred to as HKL.
[21] We are indebted to K. R. Lea for the details of the HKL calculations.
[22] S. H. Koenig, A. G. Prodell, and P. Kusch, Phys. Rev. **88**, 191 (1952).
[23] H. A. Thomas, Phys. Rev. **80**, 901 (1950).
[24] H. S. Gutowsky and R. E. McClure, Phys. Rev. **81**, 276 (1951).

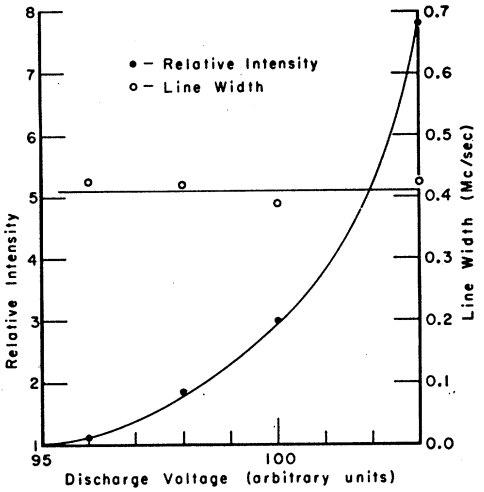

FIG. 7. Relative intensity and linewidth of a chlorine absorption line vs rf discharge voltage.

atom and atom-molecule hard-sphere collision cross sections.[3] In Fig. 7, the linewidth is shown as a function of rf discharge voltage. The atom concentration is proportional to the signal intensity. Assuming a Lorentz line shape, the linewidth due to collisions is written

$$d\nu=(1/2\pi)[V_{aa}\sigma_{aa}n_a+V_{am}\sigma_{am}n_m], \tag{7}$$

where V_{ak}=mean relative velocity, σ_{ak}=collision cross section, n_k=number/cm^3 in absorbing sample, and $k=a$ (atom) or m (molecule). Experimentally, the change in linewidth $\Delta(d\nu)$ was zero, and since the gas flow was maintained constant, the number $n=\frac{1}{2}n_a+n_m$ remained constant. Thus it is found that

$$\sigma_{am}=2V_{aa}\sigma_{aa}/V_{am}, \tag{8}$$

with the assumption that the particles in the region of observation remain at a constant temperature and in thermal equilibrium. Using the results of kinetic theory for a Maxwellian velocity distribution,

$$\sigma_{am}\simeq 2.3\sigma_{aa}. \tag{9}$$

For obtaining an absolute relation for the collision cross sections, rewrite Eq. (7) using Eq. (8):

$$\sigma_{aa}=\frac{\pi}{V_{aa}}\frac{\Delta(d\nu)}{\Delta n}. \tag{10}$$

The ratio $\Delta(d\nu)/\Delta n$ was obtained by measuring the change in linewidth as a function of pressure. This value, obtained from Fig. 8, is 2(Mc/sec)/mm. Thus

$$\sigma_{aa}=(4.1\pm 2)\times 10^{-16}\ \text{cm}^2,$$
$$\sigma_{am}=(10\pm 3)\times 10^{-16}\ \text{cm}^2.$$

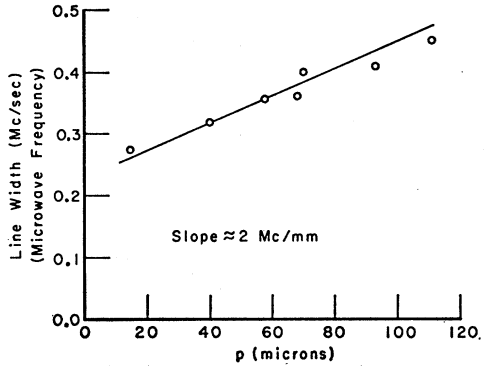

FIG. 8. Pressure broadening of a chlorine absorption line.

ACKNOWLEDGMENT

The authors gratefully acknowledge the help and encouragement given by Professor V. W. Hughes.